

# Diffractive optical elements for spectral imaging

Daniel W. Wilson, Paul D. Maker, Richard E. Muller, and Pantazis Mouroulis

Jet Propulsion Laboratory, California Institute of Technology, MS 302-231, 4800 Oak Grove Drive, Pasadena, CA 91109  
Tel: (818) 393-3548, Fax: (818) 393-4540, E-mail: [daniel.w.wilson@jpl.nasa.gov](mailto:daniel.w.wilson@jpl.nasa.gov)

Michael R. Descour, Curtis E. Volin, and Eustace L. Dereniak

Optical Sciences Center, University of Arizona, Tucson, AZ 85721  
Tel: (520) 626-5086, Fax: (520) 621-3389, E-mail: [michael.descour@opt-sci.arizona.edu](mailto:michael.descour@opt-sci.arizona.edu)

**Abstract:** Diffractive optical elements fabricated on flat and non-flat substrates frequently act as dispersive elements in imaging spectrometers. We describe the design and electron-beam fabrication of blazed and computer-generated-hologram gratings for slit and tomographic imaging spectrometers.

©2000 Optical Society of America

OCIS codes: (050.1950) Diffraction gratings, (220.4000) Microstructure fabrication

## 1. Convex blazed gratings for slit imaging spectrometers

The dispersive element in many slit imaging spectrometers is a blazed grating. In recent years, the concentric "Offner" spectrometer design (Fig. 1) has become popular due to its very low slit distortion. This design requires the grating to be fabricated on a spherical convex substrate. For high efficiency, the grating must be blazed. However, the non-flat substrate requirement makes diamond ruling difficult, and the blazing requirement makes holographic fabrication difficult. To address this need, we have developed an analog direct-write electron-beam lithography method for fabricating high-efficiency blazed gratings on convex substrates [1,2].

Since 1992, we have been using direct-write electron-beam lithography to fabricate analog-depth diffractive optics in thin films of polymethyl methacrylate (PMMA). As detailed in Ref. 3, this process involves determining the proper E-beam dose to produce a desired etch depth after acetone development. This calculation includes the experimentally determined backscattered dose from the substrate (proximity effect) and the nonlinear dose response of PMMA. For diffractive optic fabrication on non-flat (to date convex spherical) substrates, we utilize the large depth-of-field inherent in E-beam lithography. By careful calibration and testing, we have found that fabrication errors are negligible over regions that vary by  $\pm 25 \mu\text{m}$  in height. To accommodate larger height variations, the total pattern is divided into sub-patterns (annuli) with height variations of  $50 \mu\text{m}$ . Each sub-pattern is exposed using the proper settings for E-beam focus height, deflector gain, and deflector rotation. Figure 2 shows an atomic force microscope scan of a typical blazed grating.

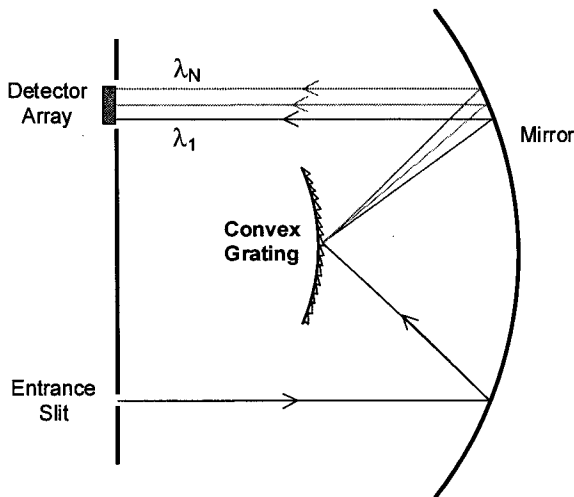


Fig. 1. Illustration of Offner imaging spectrometer form

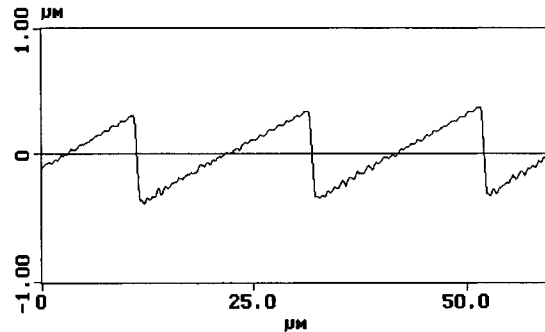


Fig. 2. Typical groove profile of an E-beam fabricated blazed grating (atomic force microscope scan)

Since 1998, we have delivered two space-qualified gratings for imaging spectrometers in flight instruments. Table I summarizes the specifications and measured performance of these gratings. For both of these instruments, the substrates were polished aluminum that we coated with 2  $\mu\text{m}$  of PMMA. After grating fabrication, we evaporated 600 $\text{\AA}$  of aluminum as the reflective surface. In all cases, the measured efficiency curve shapes matched theoretical predictions for a sawtooth groove profile.

Table 1. Specifications and performance of flight-instrument gratings

Grating	Diameter	Period	Blaze Angle	Substrate Sag	Wavelength range (order)	Peak Efficiency†, Wavelength (order)	Ghosts, Scatter‡
Spect. 1 VNIR	14 mm	17.4 $\mu\text{m}$	0.55 deg	0.23 mm	0.4 – 0.85 $\mu\text{m}$ (-1)	92% @ 490 nm	0.025%
Spect. 1 SWIR	14 mm	17.4 $\mu\text{m}$	2.27 deg	0.23 mm	1.13 – 2.55 $\mu\text{m}$ (-1)	92% @ 1450 nm	0.16%
Spect. 2 Dual-band	29 mm	35.7 $\mu\text{m}$	1.19 deg	1.27 mm	0.5 – 0.85 (-2) 1.0 – 2.45 (-1)	91% @ 0.63 $\mu\text{m}$ (-2) 93% @ 1.26 $\mu\text{m}$ (-1)	0.05%
Spect. 2 MWIR	36.6 mm	103.6 $\mu\text{m}$	1.12 deg	0	3 – 5 $\mu\text{m}$ (-1)	Not Meas.	Not Meas.

† - relative to an aluminum mirror

‡ - compared to the brightest order at 633 nm, in all cases ghosts dominated over diffuse scatter

For imaging spectrometers operating at shorter wavelengths or requiring higher dispersion, we have begun fabricating blazed gratings with smaller periods. Figure 2 shows a scanning electron microscope image of a 0.5  $\mu\text{m}$  period blazed grating (2000 lines/mm).

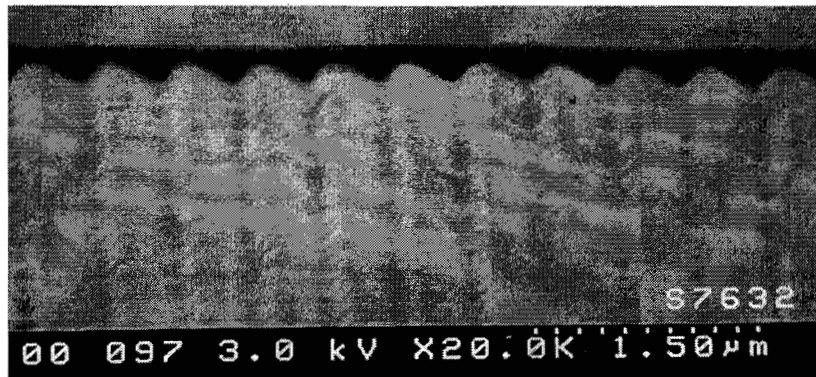


Fig. 3. SEM image of PMMA blazed grating with 0.5  $\mu\text{m}$  period.

## 2. Computer-generated hologram gratings for tomographic imaging spectrometers

In addition to traditional blazed grating profiles, we have designed and fabricated two-dimensional computer-generated hologram (CGH) gratings for computed-tomography imaging spectrometers (CTISs). The CTIS enables transient-event spectral imaging by capturing spatial and spectral information in a single image [4]. This is accomplished by imaging a scene through a 2D grating that produces multiple spectrally dispersed images. These images are simultaneously recorded by a focal plane array (FPA). From a single captured frame, tomographic reconstruction yields the spectrum of every pixel in the scene.

The two-dimensional grating in a CTIS is essentially a 1 to  $N \times N$  fan-out CGH that is designed to operate over a wide wavelength range. The grating is composed of  $M \times M$ -pixel CGH cells ( $M > N$ ) that are arrayed to fill the desired aperture. When illuminated with broadband light, the grating diffracts efficiently into  $N \times N$  orders, where the (0,0) order is an undispersed image of the scene and all other orders are dispersed radially. Figure 4 shows how a CTIS image of a scene composed of light emitting diodes and laser spots. When designing the CTIS CGH grating, the goal is to fill the FPA with dispersed information without having a single grating order saturate the image. The weighting factors of the  $N \times N$  orders of the desired fan-out are adjusted so that after dispersion, their intensities will be approximately equal. To design the broadband CGH, we have developed two methods: multiple iterative Fourier transform (IFT) [5,6] and singular value decomposition (SVD). In the multiple IFT method, we perform many IFT

single-wavelength designs of the desired  $N \times N$  CGH and evaluate the broadband performance of each using a merit function. Because the starting phase function for each design is randomly chosen, the broadband performance can vary greatly from design to design. In the singular-value decomposition technique, the desired efficiencies are specified at a number of wavelengths throughout the band. This results in an overdetermined set of equations involving the CGH pixel heights, and singular-value decomposition is used to determine the best solution. Figure 5 shows the diffraction efficiencies and dispersed FPA images of a  $5 \times 5$  equal-efficiency CGH grating designed using the SVD technique.

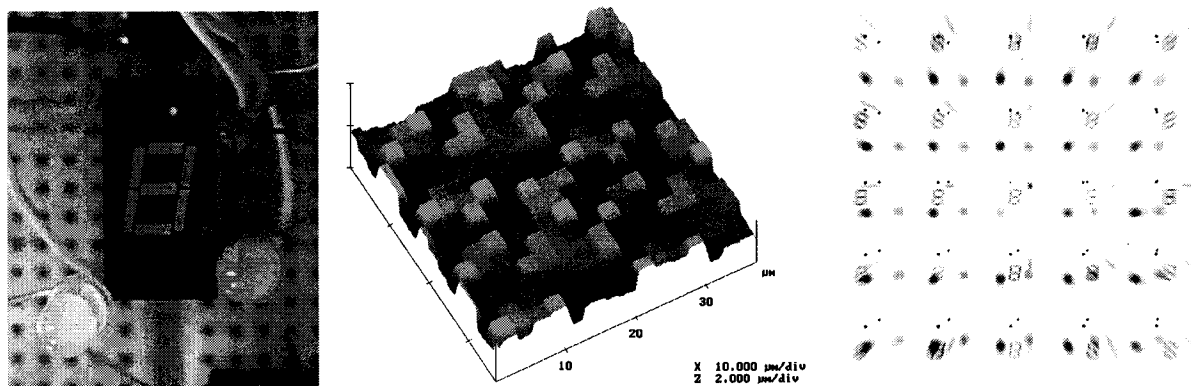


Fig. 4. Left to right: experimental scene, analog-depth E-beam fabricated CGH grating having  $2.5\mu\text{m}$  pixels (designed to produce  $5 \times 5$  non-equal efficiency orders for 450-750 nm), CTIS dispersed image using the  $5 \times 5$  CGH grating.

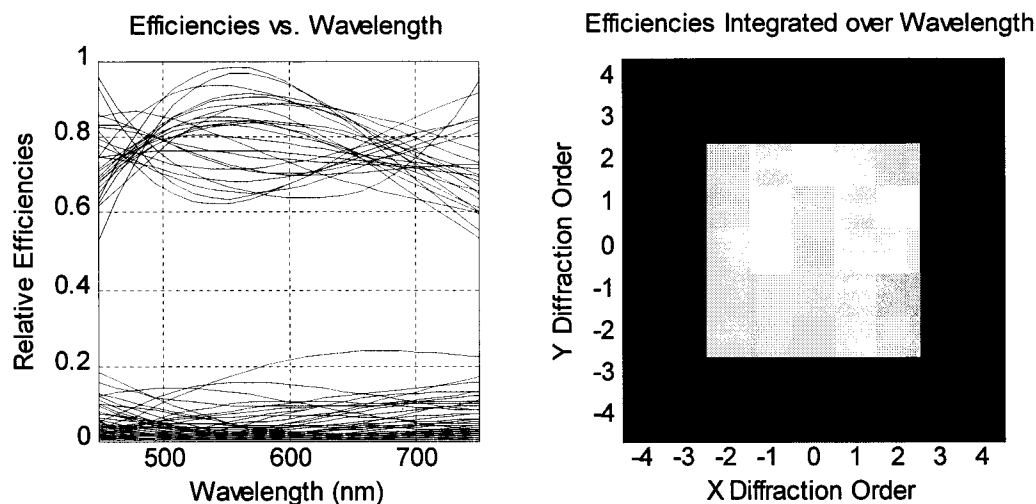


Fig. 5. Predicted relative efficiencies of an equal-efficiency  $5 \times 5$ -order CTIS CGH grating designed using the SVD method.

## 7. References

- [1] P. D. Maker, R. E. Muller, D. W. Wilson, and P. Mouroulis, "New convex grating types manufactured by electron beam lithography," 1998 OSA Diffractive Optics Topical Meeting, Kailua-Kona, Hawaii, June 8-11, 1998.
- [2] P. Mouroulis, D. W. Wilson, P. D. Maker, and R. M. Muller, "New convex grating types for concentric imaging spectrometers," *Appl. Opt.* **37**, 7200-7208 (1998).
- [3] P. D. Maker, D. W. Wilson, and R. E. Muller, "Fabrication and performance of optical interconnect analog phase holograms made by E-beam lithography," in *Optoelectronic Interconnects and Packaging*, R. T. Chen and P. S. Guilfoyle, eds., Proc. SPIE CR62, 415-430 (1996).
- [4] M. R. Descour and E. L. Dereniak, "Computed-tomography imaging spectrometer: experimental calibration and reconstruction results," *Appl. Opt.* **34**, 4817-4826 (1995).
- [5] D. W. Wilson, P. D. Maker, and R. E. Muller, "Design and Fabrication of Computer-Generated Hologram Dispersers for Computed-Tomography Imaging Spectrometers," *Optical Society of America Annual Meeting*, Oct. 1996.
- [6] M. R. Descour, C. E. Volin, T. M. Gleeson, E. L. Dereniak, M. F. Hopkins, D. W. Wilson, and P. D. Maker, "Demonstration of a computed-tomography imaging spectrometer using a computer-generated hologram disperser," *Appl. Opt.* **36**, 3694-3698 (1997).